Dong-Li Shi

Xi-Qiao Feng

Key Lab of Failure Mechanics of
Education Ministry of China,
Department of Engineering Mechanics,
Tsinghua University,
Beijing 100084,
P.R. China

Yonggang Y. Huang

Department of Mechanical and Industrial
Engineering,
University of Illinois at Urbana-Champaign,
Urbana, IL 61801

Keh-Chih Hwang

Department of Engineering Mechanics,
Tsinghua University,
Beijing 100084,
P.R. China

Huajian Gao

Max Planck Institute for Metals Research,
Heisenbergstrasse 3,
D-70569 Stuttgart, Germany

The Effect of Nanotube Waviness and Agglomeration on the Elastic Property of Carbon Nanotube-Reinforced Composites

Owing to their superior mechanical and physical properties, carbon nanotubes seem to hold a great promise as an ideal reinforcing material for composites of high-strength and low-density. In most of the experimental results up to date, however, only modest improvements in the strength and stiffness have been achieved by incorporating carbon nanotubes in polymers. In the present paper, the stiffening effect of carbon nanotubes is quantitatively investigated by micromechanics methods. Especially, the effects of the extensively observed waviness and agglomeration of carbon nanotubes are examined theoretically. The Mori-Tanaka effective-field method is first employed to calculate the effective elastic moduli of composites with aligned or randomly oriented straight nanotubes. Then, a novel micromechanics model is developed to consider the waviness or curviness effect of nanotubes, which are assumed to have a helical shape. Finally, the influence of nanotube agglomeration on the effective stiffness is analyzed. Analytical expressions are derived for the effective elastic stiffness of carbon nanotube-reinforced composites with the effects of waviness and agglomeration. It is found that these two mechanisms may reduce the stiffening effect of nanotubes significantly. The present study not only provides the relationship between the effective properties and the morphology of carbon nanotube-reinforced composites, but also may be useful for improving and tailoring the mechanical properties of nanotube composites. [DOI: 10.1115/1.1751182]

1 Introduction

Since the discovery of carbon nanotubes (CNTs) by Iijima [1], interest in CNTs has grown very rapidly because of their unique and superior properties. Both experimental and theoretical studies have shown that CNTs have extraordinary mechanical and electrical properties [2,3]. For example, numerous theoretical and experimental results have shown that both single-walled carbon nanotubes (SWCNTs) and multi-walled carbon nanotubes (MWCNTs) have Young's moduli about 1 TPa in the axial direction, depending on the diameter and chirality [4–9]. As individual molecules, CNTs are often free of defects, leading to very high tensile strength. By measuring the mechanical response of CNTs under tension, Yu et al. [6,7] obtained the tensile strength of SWCNTs ranging from 13 to 52 GPa, and reported the tensile strength of individual MWCNTs in the range from 11 to 63 GPa. Molecular dynamics and molecular mechanics calculations also predicted high tensile strengths of CNTs, much higher than carbon fibers and steels [5,10,11]. In addition, the electrical properties of CNTs are sensitively dependent on their diameters and chiralities [12,13]. Such superior properties make CNTs a very promising candidate as the ideal reinforcing fibers for advanced composites with high strength and low density. Evidently, such composites are of paramount interest in aeronautic and astronautic technology, automobile and many other modern industries.

Composites of carbon-nanotubes dispersed in metallic or polymeric matrices have attracted a considerable attention in recent years [14,15]. The effects of CNT dispersion and orientation [16], deformation mechanisms [17,18], interfacial bonding [19–21] on mechanical properties of CNT-reinforced composites have been investigated experimentally. Some CNT-reinforced composites synthesized in the laboratory seem to have good performance. Qian et al. [22] reported a MWCNT reinforced polystyrene with good dispersion and CNT-matrix adhesion. Using only 0.5 percent CNT reinforcement, the elastic modulus was improved about 40 percent over that of the matrix and the tensile strength improved about 25 percent. Pötschke et al. [23] investigated the electrical and rheological behavior of MWCNT-reinforced polycarbonate composites. They found a rapid change in the electrical resistivity and complex viscosity at about 2 percent volume fraction of CNTs due to the electrical and rheological percolation associated with interactions of CNTs. Andrews et al. [24] dispersed SWCNTs in isotropic petroleum pitch matrices and found that the tensile strength, elastic modulus, and electrical conductivity of the composite with 5 wt percent content of purified SWCNTs are enhanced by about 90 percent, 150 percent, and 340 percent, respectively. Recently, Odegard et al. [25] presented an interesting multiscale technique to calculate the effective elastic properties of CNT-reinforced polymer composites. It was found that for the composite with 1 percent CNT volume fraction, the stiffness would approach a maximum for CNT length of 60–80 nm or greater for aligned and random nanotube orientations.

Though some encouraging results have been reported, there are many other experiments that demonstrate only modest improvement in the strength and stiffness after CNTs are incorporated into polymers [2,26]. Why there are no consistent improvements in mechanical properties of CNT-reinforced composites? This is investigated in this paper and it is shown that the unsatisfactory improvement in the mechanical properties of CNT-reinforced composites could be attributed to the weak bonding between CNTs and polymer matrices as well as the waviness and agglomeration effects of CNTs. Since molecular dynamic or other atomistic models [5,27] are too computationally intensive for CNT-reinforced polymer composites, the micromechanics models are developed for the investigation of the stiffening effect of CNTs in a polymer matrix. These micromechanics models provide impor-

Contributed by the Materials Division for publication in the JOURNAL OF ENGINEERING MATERIALS AND TECHNOLOGY. Manuscript received by the Materials Division June 30, 2003; revision received March 1, 2004. Associate Editor: H. Sehitoglu.

tant property-microstructure relations for CNT-reinforced composites, particularly the effects of CNT waviness and agglomeration on the overall properties of the composites. It will be shown that both waviness and agglomeration of CNTs have significant influence on the properties of CNT-reinforced composites.

2 Straight CNTs

2.1 Composites Reinforced With Aligned, Straight CNTs. Consider a linear elastic polymer matrix reinforced by a large number of dispersed CNTs that are aligned, straight and of infinite length. Choose a representative volume element (RVE) V of the composite. The boundary ∂V of the RVE is subjected either to tractions corresponding to a uniform overall stress $\boldsymbol{\sigma}^0$ or to displacements compatible to a prescribed uniform overall strain $\boldsymbol{\varepsilon}^0$. There are many methods to estimate the overall properties of a composite [28]. We use the Mori-Tanaka method [29] in the present study because of its simplicity and accuracy even at a high volume fraction of inclusions.

The Mori-Tanaka method [29] assumes that each inclusion is embedded in an infinite pristine matrix subjected to an effective stress $\boldsymbol{\sigma}_m$ or an effective strain $\boldsymbol{\varepsilon}_m$ in the far field, where $\boldsymbol{\sigma}_m$ and $\boldsymbol{\varepsilon}_m$ denote the average stress and the average strain over the matrix, respectively. Thereby, the tensor of effective elastic moduli $\mathbf{C}$ of the composite reinforced by aligned inclusions of the same shape is given analytically by

$$\mathbf{C}=(c_m\mathbf{C}_m+c_r\mathbf{C}_r:\mathbf{A}):(c_m\mathbf{I}+c_r\mathbf{A})^{-1} \tag{1}$$

where, and throughout the paper, a boldface letter stands for a second or fourth-order tensor, and a colon between two tensors denotes contraction (inner product) over two indices; $\mathbf{I}$ is the fourth-order identity tensor; the subscripts m and r stand for the quantities of the matrix and the reinforcing phase, respectively, c_m and c_r denote the volume fractions, and $\mathbf{C}_m$ and $\mathbf{C}_r$ denote the tensors of elastic moduli of the corresponding phases; the fourth-order tensor $\mathbf{A}$ relates the average strains $\boldsymbol{\varepsilon}_r$ and $\boldsymbol{\varepsilon}_m$ via $\boldsymbol{\varepsilon}_r=\mathbf{A}:\boldsymbol{\varepsilon}_m$, and it is given by

$$\mathbf{A}=[\mathbf{I}+\mathbf{S}:(\mathbf{C}_m)^{-1}:(\mathbf{C}_r-\mathbf{C}_m)]^{-1}. \tag{2}$$

where $\mathbf{S}$ is the Eshelby tensor which is well documented in Mura's monograph [31].

We consider first a polymer composite reinforced with straight CNTs aligned in the x_2-axis direction. The matrix is assumed to be elastic and isotropic, with Young's modulus E_m and Poisson's ratio ν_m. Each straight CNT is modeled as a long fiber with transversely isotropic elastic properties. Therefore, the composite is also transversely isotropic, and its constitutive relation $\boldsymbol{\sigma}=\mathbf{C}:\boldsymbol{\varepsilon}$ can be expressed as

$$\begin{Bmatrix}\sigma_{11}\\ \sigma_{22}\\ \sigma_{33}\\ \sigma_{23}\\ \sigma_{13}\\ \sigma_{12}\end{Bmatrix}=\begin{bmatrix}k+m & l & k-m & 0 & 0 & 0\\ l & n & l & 0 & 0 & 0\\ k-m & l & k+m & 0 & 0 & 0\\ 0 & 0 & 0 & p & 0 & 0\\ 0 & 0 & 0 & 0 & m & 0\\ 0 & 0 & 0 & 0 & 0 & p\end{bmatrix}\begin{Bmatrix}\varepsilon_{11}\\ \varepsilon_{22}\\ \varepsilon_{33}\\ 2\varepsilon_{23}\\ 2\varepsilon_{13}\\ 2\varepsilon_{12}\end{Bmatrix} \tag{3}$$

where k, l, m, n, and p are Hill's elastic moduli [30]; k is the plane-strain bulk modulus normal to the fiber direction, n is the uniaxial tension modulus in the fiber direction (x_2), l is the associated cross modulus, m and p are the shear moduli in planes normal and parallel to the fiber direction, respectively.

The non-vanishing components of the Eshelby tensor $\mathbf{S}$ for a straight, long fiber along the x_2-direction is given as [31]

$$S_{1111}=S_{3333}=\frac{5-4\nu_m}{8(1-\nu_m)},\quad S_{1122}=S_{3322}=\frac{\nu_m}{2(1-\nu_m)}$$

$$S_{1133}=S_{3311}=\frac{4\nu_m-1}{8(1-\nu_m)},\quad S_{2323}=S_{1212}=\frac{1}{4}$$

$$S_{1313}=\frac{3-4\nu_m}{8(1-\nu_m)} \tag{4}$$

Its substitution into Eq. (2) leads to the non-vanishing components of $\mathbf{A}$ as

$$A_{1111}=A_{3333}=-\frac{a_3}{a_1a_2},\quad A_{1133}=A_{3311}=\frac{a_4}{a_1a_2}$$

$$A_{1122}=A_{3322}=\frac{l_r(1-\nu_m-2\nu_m^2)-E_m\nu_m}{a_1},\quad A_{2222}=1$$

$$A_{2323}=A_{1212}=\frac{E_m}{E_m+2p_r(1+\nu_m)},\quad A_{1313}=\frac{2E_m(1-\nu_m)}{a_2} \tag{5}$$

Here,

$$\begin{aligned}a_1&=(-1+2\nu_m)[E_m+2k_r(1+\nu_m)]\\ a_2&=E_m+2m_r(3-\nu_m-4\nu_m^2)\\ a_3&=E_m(1-\nu_m)\{E_m(3-4\nu_m)+2(1+\nu_m)[m_r(3-4\nu_m)\\ &\quad+k_r(2-4\nu_m)]\}\\ a_4&=E_m(1-\nu_m)\{E_m(1-4\nu_m)+2(\nu_m+1)[m_r(3-4\nu_m)\\ &\quad+k_r(2-4\nu_m)]\}\end{aligned} \tag{6}$$

and k_r, l_r, m_r, n_r, and p_r are the Hill's elastic moduli for the reinforcing phase (CNTs).

The substitution of $\mathbf{A}$ in Eq. (5) into Eq. (1) gives the tensor of effective elastic moduli of the composite reinforced by aligned, straight CNTs. In particular, the Hill's elastic moduli are found as

$$\begin{aligned}k&=\frac{E_m\{E_mc_m+2k_r(1+\nu_m)[1+c_r(1-2\nu_m)]\}}{2(1+\nu_m)[E_m(1+c_r-2\nu_m)+2c_mk_r(1-\nu_m-2\nu_m^2)]}\\ l&=\frac{E_m\{c_m\nu_m[E_m+2k_r(1+\nu_m)]+2c_rl_r(1-\nu_m^2)\}}{(1+\nu_m)[2c_mk_r(1-\nu_m-2\nu_m^2)+E_m(1+c_r-2\nu_m)]}\\ n&=\frac{E_m^2c_m(1+c_r-c_m\nu_m)+2c_mc_r(k_rn_r-l_r^2)(1+\nu_m)^2(1-2\nu_m)}{(1+\nu_m)\{2c_mk_r(1-\nu_m-2\nu_m^2)+E_m(1+c_r-2\nu_m)\}}\\ &\quad+\frac{E_m[2c_m^2k_r(1-\nu_m)+c_rn_r(1-2\nu_m+c_r)-4c_ml_r\nu_m)]}{2c_mk_r(1-\nu_m-2\nu_m^2)+E_m(1+c_r-2\nu_m)}\\ p&=\frac{E_m[E_mc_m+2(1+c_r)p_r(1+\nu_m)]}{2(1+\nu_m)[E_m(1+c_r)+2c_mp_r(1+\nu_m)]}\\ m&=\frac{E_m[E_mc_m+2m_r(1+\nu_m)(3+c_r-4\nu_m)]}{2(1+\nu_m)\{E_m[c_m+4c_r(1-\nu_m)]+2c_mm_r(3-\nu_m-4\nu_m^2)\}}\end{aligned} \tag{7}$$

Figure 1 shows the effective elastic moduli of a polystyrene composite reinforced by aligned, straight CNTs. The elastic moduli $E_\parallel$ and $E_\perp$ parallel and normal to CNTs are shown versus the volume fraction c_r of CNTs, where $E_\parallel$ and $E_\perp$ are related to Hill's elastic moduli by

$$E_\parallel=n-\frac{l^2}{k},\quad E_\perp=\frac{4m(kn-l^2)}{kn-l^2+mn} \tag{8}$$

The Young's modulus and Poisson's ratio of polystyrene are $E_m=1.9$ GPa and $\nu_m=0.3$, respectively. For the purpose of illustration, we use the following representative values of the elastic constants of SWCNTs: $n_r=450$ GPa, $k_r=30$ GPa, $m_r=p_r=1$ GPa, and $l_r=10$ GPa, which are taken from the analytical results of Popov et al. [32], who calculated the elastic moduli of CNTs. It is noted that CNTs are highly anisotropic, with Young's

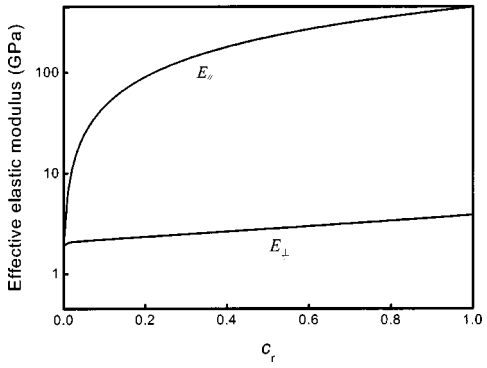

Fig. 1 A CNT with a global and a local coordinate system

modulus in the tube direction two orders of magnitude higher than that normal to the tube. It is observed from Fig. 1 that, because of CNTs' anisotropic property, the elastic modulus $E_{\parallel}$ of the composite in the CNT direction increases much more rapidly with the volume fraction c_r than $E_{\perp}$ normal to the CNT direction.

2.2 Composites Reinforced With Randomly Oriented, Straight CNTs. The effect of randomly oriented, straight CNTs is investigated in this section. The orientation of a straight CNT is characterized by two Euler angles α and β, as shown in Fig. 2. The base vectors $\mathbf{e}_i$ and $\mathbf{e}_i'$ of the global $(o-x_1x_2x_3)$ and the local coordinate systems $(o-x_1'x_2'x_3')$ are related via the transformation matrix $\mathbf{g}$

$$\mathbf{e}_i = g_{ij}\mathbf{e}_j' \tag{9}$$

where $\mathbf{g}$ is given by

$$\mathbf{g}=\begin{bmatrix} \cos\beta & -\cos\alpha\sin\beta & \sin\alpha\sin\beta \\ \sin\beta & \cos\alpha\cos\beta & -\sin\alpha\cos\beta \\ 0 & \sin\alpha & \cos\alpha \end{bmatrix} \tag{10}$$

The orientation distribution of CNTs in a composite is characterized by a probability density function $p(\alpha,\beta)$ satisfying the normalization condition

$$\int_0^{2\pi}\int_0^{\pi/2} p(\alpha,\beta)\sin\alpha\,\mathrm{d}\alpha\mathrm{d}\beta = 1 \tag{11}$$

If CNTs are completely randomly oriented, the density function is $p(\alpha,\beta)=1/2\pi$.

According to the Mori-Tanaka method, the strain $\boldsymbol{\varepsilon}_r(\alpha,\beta)$ and the stress $\boldsymbol{\sigma}_r(\alpha,\beta)$ of the CNT are related to the stress of matrix $\boldsymbol{\sigma}_m$ by

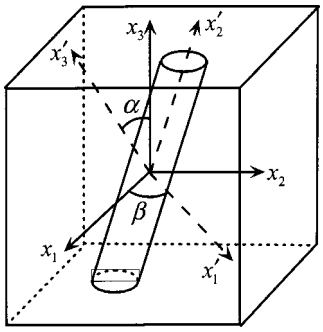

Fig. 2 Effective elastic moduli of a composite reinforced with aligned straight CNTs

$$\boldsymbol{\varepsilon}_r(\alpha,\beta)=\mathbf{A}(\alpha,\beta):\boldsymbol{\varepsilon}_m=\mathbf{A}(\alpha,\beta):\mathbf{C}_m^{-1}:\boldsymbol{\sigma}_m$$
$$\boldsymbol{\sigma}_r(\alpha,\beta)=\mathbf{C}_r:\mathbf{A}(\alpha,\beta):\boldsymbol{\varepsilon}_m=[\mathbf{C}_r:\mathbf{A}(\alpha,\beta):\mathbf{C}_m^{-1}]:\boldsymbol{\sigma}_m \tag{12}$$

where the strain concentration tensor $\mathbf{A}(\alpha,\beta)$ is given by Eq. (2). Then the average strain and stress in all randomly oriented CNTs can be written as

$$\langle\boldsymbol{\varepsilon}_r\rangle=\left[\int_0^{2\pi}\int_0^{\pi/2} p(\alpha,\beta)\mathbf{A}(\alpha,\beta)\sin\alpha\,\mathrm{d}\alpha\mathrm{d}\beta\right]:\boldsymbol{\varepsilon}_m$$
$$\langle\boldsymbol{\sigma}_r\rangle=\left[\int_0^{2\pi}\int_0^{\pi/2} p(\alpha,\beta)[\mathbf{C}_r:\mathbf{A}(\alpha,\beta):\mathbf{C}_m^{-1}]\sin\alpha\,\mathrm{d}\alpha\mathrm{d}\beta\right]:\boldsymbol{\sigma}_m \tag{13}$$

The angle brackets $\langle\square\rangle$ represent the average over special orientations. Using the average theorems $\boldsymbol{\sigma}=c_m\boldsymbol{\sigma}_m+c_r\langle\boldsymbol{\sigma}_r\rangle$ and $\boldsymbol{\varepsilon}=c_m\boldsymbol{\varepsilon}_m+c_r\langle\boldsymbol{\varepsilon}_r\rangle$ in conjunction with the effective constitutive relation $\boldsymbol{\sigma}=\mathbf{C}:\boldsymbol{\varepsilon}$, one can get the effective modulus of the composite as

$$\mathbf{C}=(c_m\mathbf{C}_m+c_r\langle\mathbf{C}_r:\mathbf{A}\rangle):(c_m\mathbf{I}+c_r\langle\mathbf{A}\rangle)^{-1} \tag{14}$$

When CNTs are completely randomly oriented in the matrix, the composite is then isotropic, and its bulk modulus K and shear modulus G are derived as

$$K=K_m+\frac{c_r(\delta_r-3K_m\alpha_r)}{3(c_m+c_r\alpha_r)},\quad G=G_m+\frac{c_r(\eta_r-2G_m\beta_r)}{2(c_m+c_r\beta_r)} \tag{15}$$

where

$$\alpha_r=\frac{3(K_m+G_m)+k_r-l_r}{3(G_m+k_r)}$$
$$\beta_r=\frac{1}{5}\left\{\frac{4G_m+2k_r+l_r}{3(G_m+k_r)}+\frac{4G_m}{G_m+p_r}+\frac{2[G_m(3K_m+G_m)+G_m(3K_m+7G_m)]}{G_m(3K_m+G_m)+m_r(3K_m+7G_m)}\right\}$$
$$\delta_r=\frac{1}{3}\left[n_r+2l_r+\frac{(2k_r+l_r)(3K_m+2G_m-l_r)}{G_m+k_r}\right]$$
$$\eta_r=\frac{1}{5}\left[\frac{2}{3}(n_r-l_r)+\frac{8G_mp_r}{G_m+p_r}+\frac{8m_rG_m(3K_m+4G_m)}{3K_m(m_r+G_m)+G_m(7m_r+G_m)}+\frac{2(k_r-l_r)(2G_m+l_r)}{3(G_m+k_r)}\right] \tag{16}$$

K_m and G_m are the bulk and shear moduli of the matrix, respectively. The effective Young's modulus E and Poisson's ratio ν of the composite are given by

$$E=\frac{9KG}{3K+G},\quad \nu=\frac{3K-2G}{6K+2G} \tag{17}$$

Figure 3 shows the effective Young's modulus versus the volume fraction of randomly oriented, straight CNTs in the same polystyrene matrix studied in Fig. 1. For comparison the Young's modulus of the same composite measured by Andrew et al. [33] is also shown in Fig. 3. It is observed that the measured Young's modulus is much smaller than the present theoretical model. Many factors may contribute to this discrepancy, such as the weak bonding between CNTs and matrices, the waviness and agglomeration of CNTs. The effects of CNT waviness and agglomeration on the effective moduli of CNT-reinforced composites are studied in the following sections.

3 Micromechanics Model for Curved CNTs

3.1 Composites Reinforced With Aligned, Curved CNTs. Experiments have shown that most CNTs in composites exist in a curved state [34,35]. This is partially because of that CNTs have very low bending stiffness due to the small tube diameter (~1

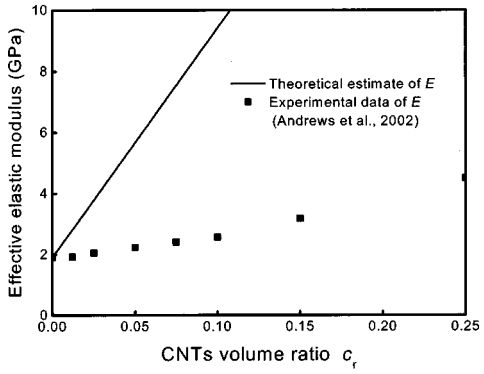

Fig. 3 Effective elastic moduli of a composite reinforced with randomly orientated straight CNTs

nm). Fisher et al. [36–38] studied numerically the effect of CNT waviness on the elastic properties of composites using the finite element method. There is yet no theoretical model to estimate the stiffening effect of curved CNTs. We will present here an analytical method to calculate the effective elastic moduli of composites containing curved CNTs.

We present in the following a micromechanics model to examine the waviness effect of curved CNTs on the elastic properties of CNT-reinforced composites. As shown in Fig. 4, a curved CNT is modeled as a helical spring, with D being the spring diameter, θ the spiral angle, and φ the polar angle. The length L of the curved CNT is related to these parameters by

$$L = \frac{\varphi D}{2\cos\theta} \tag{18}$$

The waviness of the CNT is governed by the spiral angle, θ. For example, $\theta=\pi/2$ corresponds to a straight CNT, while $\theta=0$ corresponds to a circular CNT.

The Mori-Tanaka method is employed to estimate the stiffening effect of curved CNTs. The effective elastic constitutive relation of the composite is written as

$$\overline{\boldsymbol{\sigma}} = \mathbf{C} : \overline{\boldsymbol{\varepsilon}} \tag{19}$$

where $\mathbf{C}$ is the tensor of elastic moduli of the composite and is to be determined. $\overline{\boldsymbol{\sigma}}$ and $\overline{\boldsymbol{\varepsilon}}$ denote the average stress and strain tensors in the composite, respectively, and they are related to the average stress and strain tensors $\overline{\boldsymbol{\sigma}}_m$ and $\overline{\boldsymbol{\varepsilon}}_m$ in the matrix and $\overline{\boldsymbol{\sigma}}_r$ and $\overline{\boldsymbol{\varepsilon}}_r$ in the reinforcement phase by

$$\overline{\boldsymbol{\sigma}} = c_m\overline{\boldsymbol{\sigma}}_m + c_r\overline{\boldsymbol{\sigma}}_r, \quad \overline{\boldsymbol{\varepsilon}} = c_m\overline{\boldsymbol{\varepsilon}}_m + c_r\overline{\boldsymbol{\varepsilon}}_r \tag{20}$$

Figure 5(a) shows a curved CNT embedded in a polymer matrix subjected to the average matrix stress $\overline{\boldsymbol{\sigma}}_m$ in the far field. The CNT is curved around the x_3 axis of the global system $o-x_1x_2x_3$. The RVE is divided into slices of infinitesimal thickness normal to the x_3 axis (Fig. 5(b)). The strain in the infinitesimal CNT in Fig. 5(b)

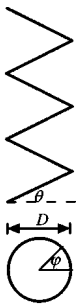

Fig. 4 The spring model of a curved CNT

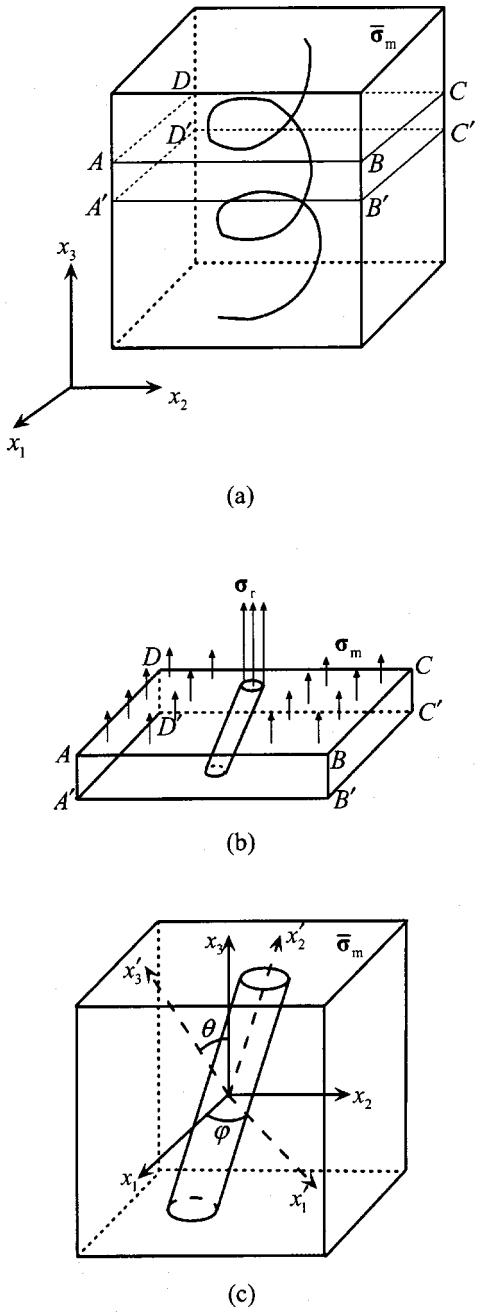

Fig. 5 Calculation model of the strain in a curved CNT: (*a*) a curved CNT in the RVE; (*b*) a slice of infinitesimal thickness; and (*c*) the approximate model for calculating the strain in the slice

is approximated by that in a long and straight CNT of the same orientation embedded in the matrix shown in Fig. 5(c), and the matrix is subjected to $\overline{\boldsymbol{\sigma}}_m$. The CNT is along the x_2' axis in the local coordinate system $o-x_1'x_2'x_3'$, with Euler angles θ and φ, where the θ is the angle between x_3 and x_3', and φ is the angle between x_1 and x_1'. The solution to this problem of a long and straight fiber has been obtained in section 2.2. It is noted that the local axis x_2' of the CNT and the x_3 axis around which the CNT is curved have a fixed angle θ, the average strain in the curved CNT is obtained by integrating with respect to the angle φ.

As shown in Fig. 5(c), the strain $\boldsymbol{\varepsilon}_r(\theta,\varphi)$ of an infinitesimal segment in the curved CNT is relate to the stress $\overline{\boldsymbol{\sigma}}_m$ by

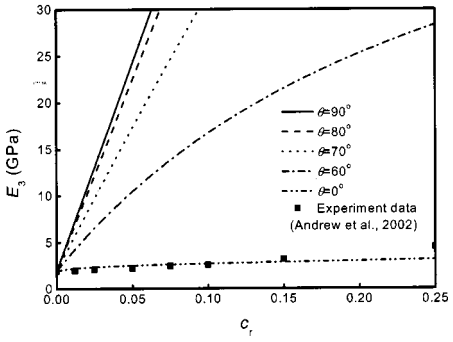

Fig. 6 Effect of CNT waviness on the effective elastic modulus in the longitudinal direction

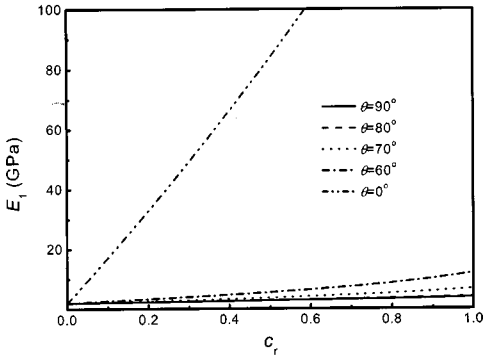

Fig. 7 Effect of CNT waviness on the effective elastic modulus in the transversal direction

$$\boldsymbol{\varepsilon}_r(\theta,\varphi)=\mathbf{A}(\theta,\varphi):\boldsymbol{\varepsilon}_m=\mathbf{A}(\theta,\varphi):\mathbf{C}_m^{-1}:\overline{\boldsymbol{\sigma}}_m \tag{21}$$

where $\mathbf{A}(\theta,\varphi)$ is the strain concentration tensor. For a curved CNT, the average strain $\overline{\boldsymbol{\varepsilon}}_r$ can be obtained from the integration of $\boldsymbol{\varepsilon}_r(\theta,\varphi)$ as

$$\overline{\boldsymbol{\varepsilon}}_r(\theta)=\frac{1}{\varphi_{\mathrm{L}}}\left[\int_0^{\varphi_L}(\mathbf{A}(\theta,\varphi):\mathbf{C}_{\mathrm{m}}^{-1})\mathrm{d}\varphi\right]:\overline{\boldsymbol{\sigma}}_{\mathrm{m}} \tag{22}$$

where φ_L is the total polar angle along the CNT. Similarly, the average stress $\overline{\boldsymbol{\sigma}}_r$ in a curved CNT is given by

$$\begin{aligned}\overline{\boldsymbol{\sigma}}_r(\theta)&=\frac{1}{\varphi_L}\left[\int_0^{\varphi_L}\mathbf{C}_r(\theta,\varphi):\boldsymbol{\varepsilon}_r(\theta,\varphi)\right]\mathrm{d}\varphi\\&=\frac{1}{\varphi_L}\left[\int_0^{\varphi_L}\mathbf{C}_r(\theta,\varphi):\mathbf{A}(\theta,\varphi):\mathbf{C}_m^{-1}\mathrm{d}\varphi\right]:\overline{\boldsymbol{\sigma}}_m\end{aligned} \tag{23}$$

The average stress and strain tensors in the composite can then be written in terms of $\overline{\boldsymbol{\sigma}}_m$ as

$$\begin{aligned}\overline{\boldsymbol{\sigma}}&=c_r\overline{\boldsymbol{\sigma}}_r+c_m\overline{\boldsymbol{\sigma}}_m=\left[\frac{c_r}{\varphi_L}\int_0^{\varphi_L}(\mathbf{C}_r(\theta,\varphi):\mathbf{A}(\theta,\varphi):\mathbf{C}_m^{-1})\mathrm{d}\varphi\right.\\&\left.+c_m\mathbf{I}\right]:\overline{\boldsymbol{\sigma}}_m\end{aligned}$$

$$\overline{\boldsymbol{\varepsilon}}=c_r\overline{\boldsymbol{\varepsilon}}_r+c_m\overline{\boldsymbol{\varepsilon}}_m=\left[\frac{c_r}{\varphi_L}\int_0^{\varphi_L}\mathbf{A}(\theta,\varphi)\mathrm{d}\varphi+c_m\mathbf{I}\right]:\mathbf{C}_m^{-1}:\overline{\boldsymbol{\sigma}}_m \tag{24}$$

The elimination of $\overline{\boldsymbol{\sigma}}_m$ in Eq. (24) gives the tensor of effective elastic moduli of the composite as

$$\begin{aligned}\mathbf{C}=&\left[\frac{c_r}{\varphi_L}\int_0^{\varphi_L}(\mathbf{C}_{\mathrm{r}}(\theta,\varphi):\mathbf{A}(\theta,\varphi):\mathbf{C}_m^{-1})\mathrm{d}\varphi\right.\\&\left.+c_m\mathbf{I}\right]:\left[\frac{c_r}{\varphi_L}\int_0^{\varphi_L}(\mathbf{A}(\theta,\varphi):\mathbf{C}_m^{-1})\mathrm{d}\varphi+c_m\mathbf{C}_m^{-1}\right]^{-1}\end{aligned} \tag{25}$$

Figure 6 shows the effective elastic modulus E_3 of the composite in the CNT axial direction (x_3) versus the volume fraction of aligned, curved CNTs in a polystyrene matrix for several spiral angles θ, where θ=90 deg corresponds to straight CNTs studied in Fig. 1, and θ=0 deg corresponds to circular CNTs. The elastic moduli of the polystyrene are the same as those in Fig. 1. For comparison, the experimental data of Andrew et al. [33] are also presented in Fig. 6, and they agree very well with the model for θ=0 deg. It is observed that the modulus E_3 in the CNT axial direction decreases rapidly as the waviness increases. For example, E_3 at θ=60 deg is less than one half of that for straight CNTs (θ=90 deg).

Figure 7 shows the effective elastic modulus $E_1(=E_2)$ of the composite normal to the CNT axial direction (i.e., x_1 or x_2) versus the volume fraction of aligned, curved CNTs in a polystyrene matrix for several spiral angles θ. Contrary to the axial moduli in Fig. 6, Fig. 7 shows that the lateral moduli $E_1(=E_2)$ increase with the waviness, even though the increase is rather small when θ changes from 90 deg to 60 deg. Therefore, we can conclude that the CNT waviness has little effect on the lateral moduli unless the spiral angle becomes very small (close to zero).

3.2 Composites Reinforced With Randomly Oriented, Curved CNTs. As in section 2.2, we introduce two angles α and β to express the orientation of a curved CNT in the composite. The orientation distribution of all CNTs is described by a probability density function $p(\alpha,\beta)$. The Mori-Tanaka method leads to the effective stiffness tensor

$$\begin{aligned}\mathbf{C}=&\left[\left\langle\frac{c_r}{\varphi_L}\int_0^{\varphi_L}(\mathbf{C}_r(\theta,\varphi):\mathbf{A}(\theta,\varphi,\alpha,\beta):\mathbf{C}_m^{-1})\mathrm{d}\varphi\right\rangle\right.\\&\left.+c_m\mathbf{I}\right]:\left[\left\langle\frac{c_r}{\varphi_L}\int_0^{\varphi_L}(\mathbf{A}(\theta,\varphi,\alpha,\beta):\mathbf{C}_m^{-1})\mathrm{d}\varphi\right\rangle+c_m\mathbf{C}_m^{-1}\right]^{-1}\end{aligned} \tag{26}$$

It is noted that the strain concentration factor $\mathbf{A}$ of a curved CNT not only depends on its orientation angles α and β but also is nonuniform within the same CNT. Therefore, it is a function of four angles, α, β, θ, and φ. For general cases of CNTs orientations, the effective elastic tensor of a CNT-reinforced composite can be determined from Eq. (26) provided that the orientation distribution function has been known.

In the case of completely random orientations of CNTs, the composite will be isotropic. Interestingly, it is found that for this special case, the present model for curved CNTs leads to the same results as Eq. (15). That is, the waviness of CNTs does not influence the effective elastic moduli of composites reinforced with randomly oriented CNTs.

4 Agglomeration of CNTs

4.1 A Two-Parameter Model of Agglomeration. CNTs have low bending stiffness (due to small diameter and small elastic modulus in the radial direction) and high aspect ratio, which make CNTs easy to agglomerate in a polymer matrix [34,35]. In order to achieve the desired properties of CNT-reinforced composites, it is critical to make CNTs uniformly dispersed in the matrix [39]. We develop a micromechanics model in this section to study the influence of the agglomeration of CNTs on the effective elastic moduli of CNT-reinforced composites.

Stephan et al. [40] observed that in the 7.5 percent concentration sample, a large amount of CNTs are concentrated in aggregates. The spatial distribution of CNTs in the matrix is nonuniform such that some local regions have a higher concentration of CNTs than the average volume fraction in the material. These

regions with concentrated CNTs are assumed in this section to have spherical shapes, and are considered as "inclusions" with different elastic properties from the surrounding material, as shown in Fig. 8. The total volume V_r of CNTs in the RVE V can be divided into the following two parts:

$$V_r = V_r^{\text{inclusion}} + V_r^m \tag{27}$$

where $V_r^{\text{inclusion}}$ and V_r^m denote the volumes of CNTs dispersed in the inclusions (concentrated regions) and in the matrix, respectively.

Introduce two parameters ξ and ζ to describe the agglomeration of CNTs

$$\xi = \frac{V_{\text{inclusion}}}{V}, \quad \zeta = \frac{V_r^{\text{inclusion}}}{V_{\text{r}}} \tag{28}$$

where $V_{\text{inclusion}}$ is the volume of the sphere inclusions in the RVE. ξ denotes the volume fraction of inclusions with respect to the total volume V of the RVE. When $\xi=1$, nanotubes are uniformly dispersed in the matrix, and with the decrease in ξ, the agglomeration degree of CNTs is more severe. The parameter ζ denotes the volume ratio of nanotubes that are dispersed in inclusions and the total volume of the nanotubes. When $\zeta=1$, all the nanotubes are located in the sphere areas. In the case where all nanotubes are dispersed uniformly, one has that $\zeta=\xi$. The bigger the value ζ with $\zeta>\xi$, the more heterogeneous the spatial distribution of CNTs.

The average volume fraction c_r of CNTs in the composite is

$$c_r = \frac{V_r}{V} \tag{29}$$

Using Eqs. (27)–(29), the volume fractions of CNTs in the inclusions and in the matrix are expressed, respectively, as

$$\frac{V_r^{\text{inclusion}}}{V_{\text{inclusion}}} = \frac{c_r\zeta}{\xi}, \quad \frac{V_r^m}{V - V_{\text{inclusion}}} = \frac{c_r(1-\zeta)}{1-\xi} \tag{30}$$

Thus, we consider the CNT-reinforced composite as a system consisting of inclusions of sphere shape embedded in a hybrid matrix. Both the matrix and the inclusions contain CNTs. We may first estimate respectively the effective elastic stiffness of the inclusions and the matrix, and then calculate the overall property of the whole composite system.

The effective elastic moduli of the hybrid inclusions and the matrix can be calculated by different micromechanics methods. Assume that all the orientations of the CNTs are completely random. We will use two methods to estimate the elastic property of the inclusions and matrix. First, the Voigt model provides the effective modulus of inclusions E_{in} and their surrounding E_{out} as [41]

$$\begin{aligned} E_{\text{out}} &= \frac{3}{8}\left\{\frac{c_r(1-\zeta)}{1-\xi}E_{\text{CNT}} + \left[1 - \frac{c_r(1-\zeta)}{1-\xi}\right]E_m\right\} \\ &\quad + \frac{5}{8}\left\{\frac{(1-\xi)E_{\text{CNT}}E_m}{[(1-\xi)-c_r(1-\zeta)]E_{\text{CNT}} + c_r(1-\zeta)E_m}\right\} \\ E_{\text{in}} &= \frac{3}{8\xi}[c_r\zeta E_{\text{CNT}} + (\xi - c_r\zeta)E_m] + \frac{5}{8}\frac{\xi E_m E_{\text{CNT}}}{(\xi - c_r\zeta)E_{\text{CNT}} + c_r\zeta E_m} \end{aligned} \tag{31}$$

where both the matrix and the CNTs are considered to be isotropic, with Young's moduli E_m and E_{CNT}, respectively. That is, the influence of anisotropy of CNTs is neglected.

In the second method, we assume the nanotubes are transversely isotropic. The elastic moduli of the hybrid matrix are estimated by the Mori-Tanaka method, as described in section 2.2. It is assumed that the CNTs are randomly oriented in the inclusions, and, therefore, the inclusions are isotropic. The effective bulk moduli K_{in} and K_{out} and the effective shear moduli G_{in} and G_{out} of the inclusions and the matrix are given, respectively, by

$$\begin{aligned} K_{\text{in}} &= K_m + \frac{(\delta_r - 3K_m\alpha_r)c_r\zeta}{3(\xi - c_r\zeta + c_r\zeta\alpha_r)}, \\ K_{\text{out}} &= K_m + \frac{c_r(\delta_r - 3K_m\alpha_r)(1-\zeta)}{3[1-\xi - c_r(1-\zeta) + c_r(1-\zeta)\alpha_r]} \\ G_{\text{in}} &= G_m + \frac{c_r\zeta(\eta_r - 2G_m\beta_r)}{2(\xi - c_r\zeta + c_r\zeta\beta_r)} \\ G_{\text{out}} &= G_m + \frac{c_{\text{r}}(1-\zeta)(\eta_{\text{r}} - 2G_m\beta_r)}{2[1-\xi - c_r(1-\zeta) + c_r(1-\zeta)\beta_r]} \end{aligned} \tag{32}$$

For a sphere inclusion in an isotropic matrix, the Eshelby's tensor read

$$\begin{aligned} S_{1111} &= S_{2222} = S_{3333} = \frac{7 - 5\nu_{\text{out}}}{15(1-\nu_{\text{out}})} \\ S_{1122} &= S_{2233} = S_{3311} = -\frac{1 - 5\nu_{\text{out}}}{15(1-\nu_{\text{out}})} \\ S_{1212} &= S_{2323} = S_{3131} = \frac{4 - 5\nu_{\text{out}}}{15(1-\nu_{\text{out}})} \end{aligned} \tag{33}$$

where $\nu_{\text{out}} = (3K_{\text{out}} - 2G_{\text{out}})/2(3K_{\text{out}} + G_{\text{out}})$ is the Poisson's ratio of the hybrid matrix.

Finally, the effective bulk modulus K and the effective shear modulus G of the composite are derived from the Mori-Tanaka method as

$$\begin{aligned} K &= K_{\text{out}}\left[1 + \frac{\xi\left(\frac{K_{\text{in}}}{K_{\text{out}}} - 1\right)}{1 + \alpha(1-\xi)\left(\frac{K_{\text{in}}}{K_{\text{out}}} - 1\right)}\right] \\ G &= G_{\text{out}}\left[1 + \frac{\xi\left(\frac{G_{\text{in}}}{G_{\text{out}}} - 1\right)}{1 + \beta(1-\xi)\left(\frac{G_{\text{in}}}{G_{\text{out}}} - 1\right)}\right] \end{aligned} \tag{34}$$

with $\alpha = (1+\nu_{\text{out}})/3(1-\nu_{\text{out}})$ and $\beta = 2(4-5\nu_{\text{out}})/15(1-\nu_{\text{out}})$.

4.2 Examples and Discussions

4.2.1 Complete Agglomeration of CNTs ($\zeta=1$). Consider first the extreme case of agglomeration where all CNTs are concentrated in spherical subregions, i.e., $\zeta=1$. Thus the above two-parameter agglomeration model is reduced to have only one agglomeration parameter, ξ. Then, the local volume fraction of CNTs in the "inclusions," which are, in turn, embedded in the pristine polymer matrix, is written as

$$\frac{V_r}{V_{\text{inclusion}}} = \frac{c_r}{\xi} \tag{35}$$

If the influence of anisotropy of CNTs is omitted and their elastic property is described by the Young's modulus E_r and Poisson's ratio ν_r, the effective moduli of the composite with agglomerated CNTs can be estimated by Eq. (31). We take the representative values of CNTs and matrix as $E_r = 450$ GPa, $E_m = 1.9$ GPa, and $\nu_r = \nu_m = 0.3$. Under different average contents c_r of CNTs in the material, the effective Young's modulus is plotted in Fig. 9(a) with respect to the agglomeration parameter ξ. When the CNTs are uniformly dispersed in the composite, i.e., $\xi=1$, the effective Young's modulus has the maximum value. With the decrease in the agglomeration parameter ξ from unity, the effective stiffness decreases very rapidly. When $\xi<0.6$, the addition of CNTs does not yield an evident stiffening effect.

If the CNTs are considered to be transversely isotropic, the effective elastic moduli of the composite can be determined by Eqs. (17), (32), and (34). Take the elastic constants of CNTs and

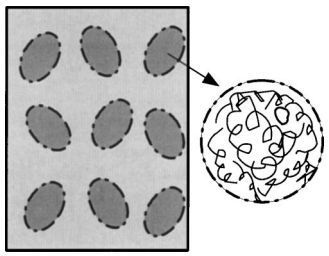

Fig. 8 Eshelby inclusion model of agglomeration of CNTs

matrix as in section 2.1. The changing curves of the effective tensile moduli with the agglomeration parameter ξ are given in Fig. 9(b). It is also clearly shown that the agglomeration of CNTs exerts a significant weakening effect to CNT-reinforced composites. In addition, it is seen by comparing (a) and (b) that the anisotropic property of CNTs affects to a considerable extent the overall effective elastic modulus, especially the maximum Young's modulus at uniform distribution. In other words, the isotropy assumption of CNTs will lead to an overestimation of the effective tensile modulus.

4.2.2 Partial Agglomeration of CNTs. In more general cases, both the parameters ζ and ξ are required to describe the agglomeration of CNTs. The former stands for the relative amount of CNTs that are concentrated in local regions or ''inclusions,'' and the latter presents the volume fraction of these inclusions in the composite.

If the CNTs are considered isotropic, the effective Young's moduli are shown in Fig. 10(a) in which ξ=0.5. It is seen that

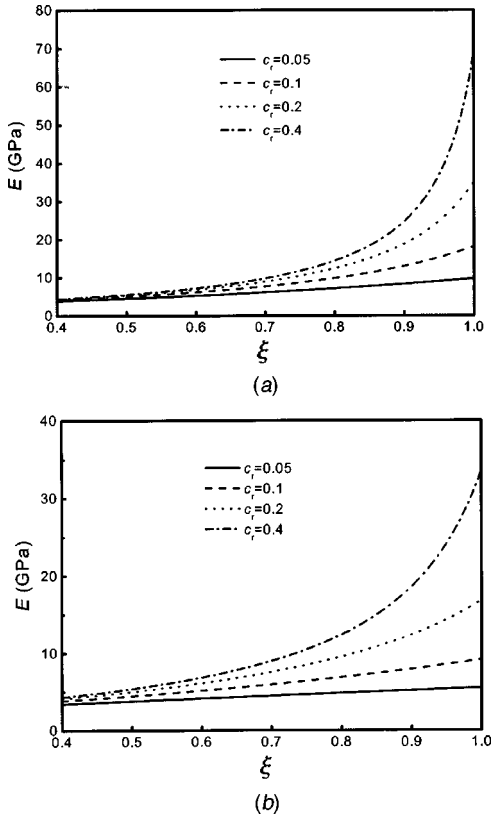

Fig. 9 Effect of CNT agglomeration on the effective elastic modulus with ζ=1, in which the CNTs are assumed to be: (*a*) isotropic; and (*b*) transversely isotropic

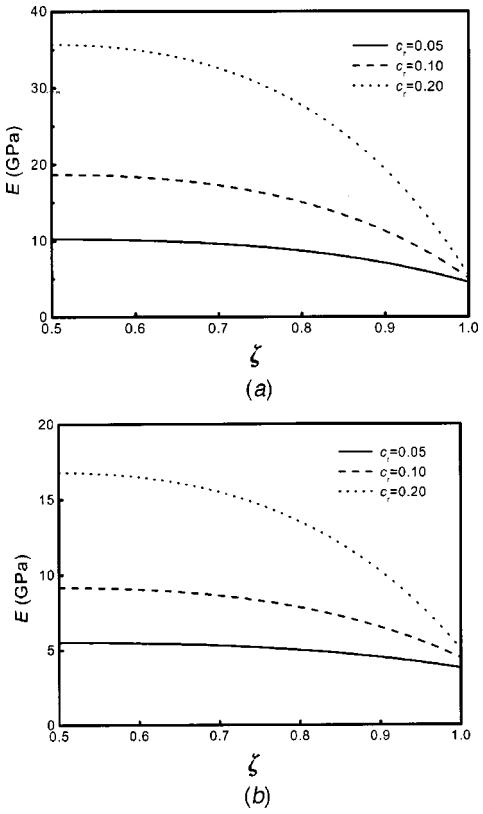

Fig. 10 The effective elastic modulus of a CNT-reinforced composite with agglomeration effect with ξ=0.5, in which the CNTs are assumed to be: (*a*) isotropic; and (*b*) transversely isotropic

with the increase in the relative amount ζ of the CNTs that are agglomerated in the inclusions, the effective Young's modulus of the composite decreases rapidly.

When the CNTs are considered to be transversely isotropic, the effective Young's moduli with respect to the agglomeration parameter ζ are shown in Fig. 10(b) with ξ=0.5. The curves in Fig. 10(b) have the similar changing tendency but are smaller in the stiffening magnitude. It is concluded from Fig. 10 that the agglomeration of CNTs exerts a pronounced weakening effect to the effective elastic property of CNT-reinforced composites, and that neglecting the anisotropic property of CNTs will cause an overestimation of the effective stiffness of composites.

5 Concluding Remarks

In the present paper, the effects of the widely observed waviness and agglomeration of carbon nanotubes are examined theoretically by using analytical micromechanics methods. A novel model is suggested to consider the waviness or curviness effect of CNTs, which are assumed to have a spiral shape. The influence of agglomeration of CNTs on the effective stiffness is analyzed by using an Eshelby's inclusion model, where the composite is assumed to have spherical inclusions with concentrated CNTs. It is established that these two mechanisms may significantly reduce the stiffening effect of CNTs. The present study not only provides the important relationship between the effective properties and the morphology of CNT-reinforced composites, but also may be useful for improving and tailoring their mechanical properties. The obtained results indicate that a CNT-reinforced composite can possibly reach superior mechanical properties only if the CNTs are controlled to have a straight shape and to be dispersed uniformly in the whole material [42]. These high requirements are by no means easy to be satisfied, but considerable developments have

been made in this field by researchers of materials science and it is believable that CNT-reinforced composites will play a significant role in various modern industries in the near future.

Acknowledgment

X.-Q. Feng acknowledges the support from the National Natural Science Foundation of China (NSFC Grant No. 10028204, 90305025 and 10102008), the Education Ministry of China (National Distinguished Doctoral Dissertation Funding Grant Nr. 199926, and Grant Key Project Nr. 0306), and 973 Program (Nr. 2003CB615603). Y. Huang acknowledges the support from ONR (Grant No. 00014-01-1-0205, Program Officer Dr. Y. D. S. Yajakapse), NSF (Grants No. 0099909 and No. 0103257), Alexander von Humboldt Foundation, Center for Advanced Study at UIUC, NCSA Faculty Fellows Program, and NSFC.

References

[1] Iijima, S., 1991, ''Helical Microtubles of Graphitic Carbon,'' Nature (London), **354**, pp. 56–58.
[2] Qian, D., Wagner, G. J., Liu, W. K., Yu, M. F., and Ruoff, R. S., 2002, ''Mechanics of Carbon Nanotubes,'' Appl. Mech. Rev., **55**(6), pp. 495–533.
[3] Saito, R., Dresselhaus, G., and Dresselhaus, M. S., 1998, *Physical Properties of Carbon Nanotubes*, Imperial College Press, London.
[4] Treacy, M. M. J., Ebbesen, T. W., and Gibson, J. M., 1996, ''Exceptionally High Young's Modulus Observed for Individual Carbon Nanotubes,'' Nature (London), **381**, pp. 678–680.
[5] Yakobson, B. I., Brabec, C. J., and Bernholc, J., 1996, ''Nanomechanics of Carbon Tubes: Instability Beyond Linear Response,'' Phys. Rev. Lett., **76**(14), pp. 2511–2514.
[6] Yu, M. F., Files, B. S., Arepalli, S., and Ruoff, R. S., 2000, ''Tensile Loading of Ropes of Single Wall Carbon Nanotubes and Their Mechanical Properties,'' Phys. Rev. Lett., **84**, pp. 5552–5555.
[7] Yu, M. F., Lourie, O., Dyer, M. J., Moloni, K., and Ruoff, R. S., 2000, ''Strength and Breaking Mechanism of Multiwalled Carbon Nanotubes Under Tensile Load,'' Science, **287**, pp. 637–640.
[8] Zhang, P., Huang, Y., Gao, H., and Hwang, K. C., 2002, ''Fracture Nucleation in Single-Wall Carbon Nanotubes Under Tension: A Continuum Analysis Incorporating Interatomic Potentials,'' ASME J. Appl. Mech., **69**(3), pp. 454–458.
[9] Zhang, P., Huang, Y., Geubelle, P. H., Klein, P. A., and Hwang, K. C., 2002, ''The Elastic Modulus of Single-Wall Carbon Nanotubes: A Continuum Analysis Incorporating Interatomic Potentials,'' Int. J. Solids Struct., **39**, pp. 3893–3906.
[10] Cornwell, C. F., and Wille, L. T., 1997, ''Elastic Properties of Single-Walled Carbon Nanotubes in Compression,'' Solid State Commun., **101**(8), pp. 555–558.
[11] Yao, Z. H., Zhu, C. C., Cheng, M., and Liu, J., 2001, ''Mechanical Properties of Carbon Nanotube by Molecular Dynamics Simulation,'' Comput. Mater. Sci., **22**, pp. 180–184.
[12] Ebbesen, T. W., Lezec, H. J., and Hiura, H., 1996, ''Electrical Conductivity of Individual Carbon Nanotubes,'' Nature (London), **382**, pp. 54–56.
[13] Wei, J. H., Xie, S. J., Wang, S. G., and Mei, M. L., 2001, ''Dimensional Model of Carbon Nanotubes,'' Phys. Lett. A, **292**, pp. 207–211.
[14] Calvert, P., 1999, ''Nanotube Composites: A Recipe for Strength,'' Nature (London), **399**, pp. 210–211.
[15] Thostenson, E. T., Ren, Z., and Chou, T. W., 2001, ''Advances in the Science and Technology of Carbon Nanotubes and Their Composites: A Review,'' Compos. Sci. Technol., **61**, pp. 1899–1912.
[16] Haggenmueller, R., Gommans, H. H., Rinzler, A. G., Fischer, J. E., and Winey, K. I., 2000, ''Aligned Single-Wall Carbon Nanotubes in Composites by Melt Processing Methods,'' Chem. Phys. Lett., **330**, pp. 219–225.
[17] Bower, C., Rosen, R., Jin, L., Han, J., and Zhou, O., 1999, ''Deformation of Carbon Nanotubes in Nanotube-Polymer Composites,'' Appl. Phys. Lett., **74**(22), pp. 3317–3319.
[18] Lourie, O., Cox, D. M., and Wagner, H. D., 1998, ''Buckling and Collapse of Embedded Carbon Nanotubes,'' Phys. Rev. Lett., **81**(8), pp. 1638–1641.
[19] Wagner, H. D., Lourie, O., Feldman, Y., and Tenne, R., 1998, ''Stress-Induced Fragmentation of Multiwall Carbon Nanotubes in a Polymer Matrix,'' Appl. Phys. Lett., **72**(2), pp. 188–190.
[20] Lourie, O., and Wagner, H. D., 1998, ''Transmission Electron Microscopy Observations of Single-Wall Carbon Nanotubes Under Axial Tension,'' Appl. Phys. Lett., **73**(24), pp. 3527–3529.
[21] Jia, Z. J., Wang, Z., Xu, C., Liang, J., Wei, B., Wu, D., and Zhu, S., 1999, ''Study on Poly(methyl methacrylate)/Carbon Nanotube Composites,'' Mater. Sci. Eng., A, **271**, pp. 395–400.
[22] Qian, D., Dickey, E. C., Andrews, R., and Rantell, T., 2000, ''Load Transfer and Deformation Mechanisms in Carbon Nanotube-Polystyrene Composites,'' Appl. Phys. Lett., **76**, pp. 2868–2870.
[23] Pötschke, P., Fornes, T. D., and Paul, D. R., 2002, ''Rheological Behavior of Multiwalled Carbon Nanotube/Polycarbonate Composites,'' Polymer, **43**(11), pp. 3247–3255.
[24] Andrews, R., Jacques, D., Rao, A. M., Rantell, T., Derbyshire, F., Chen, Y., Chen, J., and Haddon, R. C., 1999, ''Nanotube Composite Carbon Fibers,'' Appl. Phys. Lett., **75**(9), pp. 1329–1331.
[25] Odegard, G. M., Gates, T. S., Wise, K. E., Park, C., and Siochi, E. J., 2002, ''Constitutive Modeling of Nanotube-Reinforced Polymer Composites,'' Compos. Sci. Technol., **63**(11), pp. 1671–1687.
[26] Ajayan, P. M., Schadler, L. S., Giannaris, C., and Rubio, A., 2000, ''Single-Walled Nanotube-Polymer Composites: Strength and Weaknesses,'' Adv. Mater. (Weinheim, Ger.), **12**(10), pp. 750–753.
[27] Nardelli, M. B., Fattebert, J. L., Orlikowski, D., Roland, C., Zhao, Q., and Bernholc, J., 2000, ''Mechanical Properties, Defects and Electronic Behavior of Carbon Nanotubes,'' Carbon, **38**, pp. 1703–1711.
[28] Nemat-Nasser, S., and Hori, M., 1993, *Micromechanics: Overall Properties of Heterogeneous Materials*, North-Holland, New York.
[29] Mori, T., and Tanaka, K., 1973, ''Average Stress in Matrix and Average Elastic Energy of Materials With Misfitting Inclusions,'' Acta Metall., **21**, pp. 571–574.
[30] Hill, R., 1965, ''A Self-Consistent Mechanics of Composite Materials,'' J. Mech. Phys. Solids, **13**, pp. 213–222.
[31] Mura, T., 1987, *Micromechanics of Defects in Solids*, Martinus Nijhoff Publishers, Dordrecht.
[32] Popov, V. N., Doren, V. E., and Balkanski, M., 2000, ''Elastic Properties of Crystals of Single-Walled Carbon Nanotubes,'' Solid State Commun., **114**, pp. 395–399.
[33] Andrews, R., Jacques, D., Minot, M., and Rantell, T., 2002, ''Fabrication of Carbon Multiwall Nanotube/Polymer Composites by Shear Mixing,'' Macromolecular Materials and Engineering, **287**, pp. 395–403.
[34] Shaffer, M. S. P., and Windle, A. H., 1999, ''Fabrication and Characterization of Carbon Nanotube/Poly(vinyl alcohol) Composites,'' Adv. Mater. (Weinheim, Ger.), **11**, pp. 937–941.
[35] Vigolo, B., Penicaud, A. P., Couloun, C., Sauder, S., Pailler, R., Journet, C., Bernier, P., and Poulin, P., 2000, ''Macroscopic Fibers and Ribbons of Oriented Carbon Nanotubes,'' Science, **290**, pp. 1331–1334.
[36] Fisher, F. T., Bradshaw, R. D., and Brinson, L. C., 2002, ''Effects of Nanotube Waviness on the Modulus of Nanotube-Reinforced Polymers,'' Appl. Phys. Lett., **80**(24), pp. 4647–4649.
[37] Fisher, F. T., Bradshaw, R. D., and Brinson, L. C., 2003, ''Fiber Waviness in Nanotube-Reinforced Polymer Composites: I. Modulus Predictions Using Effective Nanotube Properties,'' Compos. Sci. Technol., **63**(11), pp. 1689–1703.
[38] Bradshaw, R. D., Fisher, F. T., and Brinson, L. C., 2003, ''Fiber Waviness in Nanotube-Reinforced Polymer Composites: II. Modeling via Numerical Approximation of the Dilute Strain Concentration Tensor,'' Compos. Sci. Technol., **63**(11), pp. 1705–1722.
[39] Curtin, W. A., 2002, private communication with Y. Huang.
[40] Stephan, C., Nguyen, T. P., Chapelle, M. L., and Lefrant, S., 2000, ''Characterization of Single-Walled Carbon Nanotubes-PMMA Composite,'' Synth. Met., **108**, pp. 139–149.
[41] Jones, R. M., 1999, *Mechanics of Composite Materials*, Taylor & Francis, Philadelphia.
[42] Shi, D. L., Feng, X. Q., Huang, Y., and Hwang, K. C., 2004, ''Critical evaluation of the stiffening effect of carbon nanotubes in composites,'' Key Eng. Mater., **261–263**, pp. 1487–1492.